Hindawi Publishing Corporation
BioMed Research International
Volume 2014, Article ID 209398, 15 pages
http://dx.doi.org/10.1155/2014/209398

*Research Article*

# Dipeptidyl Peptidase 10 ($DPP10_{789}$): A Voltage Gated Potassium Channel Associated Protein Is Abnormally Expressed in Alzheimer's and Other Neurodegenerative Diseases

**Tong Chen,[1] Wei-Ping Gai,[2] and Catherine A. Abbott[1]**

[1] *School of Biological Sciences, Flinders University, GPO Box 2100, Adelaide, SA 5001, Australia*
[2] *Department of Human Physiology, School of Medicine, Flinders University, GPO Box 2100, Adelaide, SA 5001, Australia*

Correspondence should be addressed to Catherine A. Abbott; cathy.abbott@flinders.edu.au

Received 13 January 2014; Accepted 23 April 2014; Published 16 June 2014

Academic Editor: Hanna Rosenmann



The neuropathological features associated with Alzheimer's disease (AD) include the presence of extracellular amyloid-$\beta$ peptide-containing plaques and intracellular tau positive neurofibrillary tangles and the loss of synapses and neurons in defined regions of the brain. Dipeptidyl peptidase 10 (DPP10) is a protein that facilitates Kv4 channel surface expression and neuronal excitability. This study aims to explore $DPP10_{789}$ protein distribution in human brains and its contribution to the neurofibrillary pathology of AD and other tauopathies. Immunohistochemical analysis revealed predominant neuronal staining of $DPP10_{789}$ in control brains, and the CA1 region of the hippocampus contained strong reactivity in the distal dendrites of the pyramidal cells. In AD brains, robust $DPP10_{789}$ reactivity was detected in neurofibrillary tangles and plaque-associated dystrophic neurites, most of which colocalized with the doubly phosphorylated Ser-202/Thr-205 tau epitope. $DPP10_{789}$ positive neurofibrillary tangles and plaque-associated dystrophic neurites also appeared in other neurodegenerative diseases such as frontotemporal lobar degeneration, diffuse Lewy body disease, and progressive supranuclear palsy. Occasional $DPP10_{789}$ positive neurofibrillary tangles and neurites were seen in some aged control brains. Western blot analysis showed both full length and truncated $DPP10_{789}$ fragments with the later increasing significantly in AD brains compared to control brains. Our results suggest that $DPP10_{789}$ is involved in the pathology of AD and other neurodegenerative diseases.

## 1. Introduction

Alzheimer's disease (AD) is a progressive neurodegenerative disorder characterized pathologically by the presence of extracellular amyloid plaques containing the amyloid-$\beta$ peptide (A$\beta$) and intracellular neurofibrillary tangles (NFTs) containing hyperphosphorylated microtubule-associated protein tau and loss of synapses and neurons in select brain regions [1–3]. The aetiology of AD is complex, with a majority of cases being sporadic and approximately 10% being inherited. Mutations have been identified in genes encoding amyloid precursor protein (APP) [4, 5], presenilin 1 (PS1), and PS2 in a small subset of familial AD cases. In sporadic AD cases, polymorphisms of apolipoprotein E4 and other genes have been associated with an increased risk of developing the disease [6].

Oxidative stress, impaired energy metabolism, and disruption of neuronal $Ca^{2+}$ regulation have all been implicated in the cellular pathophysiology. Although experimental approaches indicate that A$\beta$ deposition plays an important role in the neurodegenerative process in AD [7, 8], the mechanism underlying the relentless progression of neurofibrillary pathology and neuronal death remains to be fully elucidated. Over the last decade there have been a number of studies demonstrating that potassium channel dysfunction may be involved in the pathogenesis of AD [9–13].

Neuronal excitability is finely controlled by various membranous channels and associated proteins. In the central nervous system, the rapidly inactivating voltage-gated potassium channels (Kv channels) are the major determinants of dendritic excitability [14]. In particular, Kv4 channels, a subfamily of Kv channels, account for a large portion of the

Table 1: Primary antibodies used in this study.

| Antibody/antiserum | Species | Epitope | Source | Dilution |
|---|---|---|---|---|
| $DPP10_{789}$ (polyclonal) | Rabbit | $DPP10_{789}$ $N$-terminal intracellular domain | This lab | 1 : 100 |
| Anti-GFP (polyclonal) | Rabbit | GFP | Invitrogen, USA | 1 : 3000 |
| AT8 | Mouse | Specific for tau phosphorylation at Ser 202 and/or Thr 205 | Innogenetics, Belgium | 1 : 1000 |
| Tau2 | Mouse | Phosphorylated and nonphosphorylated tau | Novocastra, UK | 1 : 1000 |
| A4 | Mouse | $\beta$-Amyloid | Professor Colin Masters, Melbourne University | 1 : 250 |
| Anti-$\beta$III-tubulin monoclonal Ab | Mouse | $C$-Terminus of $\beta$III-tubulin | Promega, USA | 1 : 10000 |

somatodendritic inactivating current in neurons in regulating firing frequency and signal processing in dendrites. The Kv4 channels are composed of the pore-forming subunits, various auxiliary subunits, and other interacting proteins such as Kv channel interacting proteins and dipeptidyl peptidase-like proteins DPP6 and DPP10 [15–17].

Indeed, potassium channel dysfunction has been demonstrated in fibroblasts and platelets of AD patients [9, 10]. Postmortem studies have also showed alterations of potassium channel expression in AD brains [18]. Several publications have demonstrated that A$\beta$ is involved in Kv channel function and may even play a physiological role in controlling neuronal excitability [19, 20]. In addition, Kv channel interacting protein 3, also known as calsenilin, is a presenilin binding protein [21] that preferentially interacts with the familial AD associated $C$-terminal fragment of PS2 [22]. Moreover, the application of A$\beta$ peptide to cultured cells increases both Kv channel interacting protein 3 mRNA and protein expression as well as cell death. The A$\beta$ toxicity can be prevented by blocking expression of Kv channel interacting protein 3 [23]. Furthermore, in a study using a transgenic model of Alzheimer's disease, some potassium channels in hippocampal neurons were found to be absent [24]. Liu et al. reported that a potassium channel activator diazoxide ameliorated A$\beta$ and tau pathologies and improves memory in the 3xTg AD mouse model [25]. Thus there is a body of research that suggests that potassium channels or their associated proteins might be involved in steps leading to the neurodegeneration observed in AD.

DPP10 belongs to the dipeptidyl peptidase 4 (DPP4) gene family sharing 59% amino acid sequence similarity with DPP4, an atypical serine protease [26, 27]. However DPP10 is missing the nucleophilic Ser residue in the catalytic motif and lacks enzyme activity. So far, four splice variants have been reported for DPP10. As a result of alternate splicing of the first exon, each variant has a short divergent cytoplasmic $N$-terminus. The remaining protein of each variant is identical and consists of a highly conserved juxtamembrane, transmembrane, and large extracellular $C$-terminal domain. Kv4 channels containing different DPP10 variants display distinct inactivation kinetics and voltage dependence at depolarized potentials, indicating that the cytoplasmic portion of the DPP10 protein influences the inactivation properties [28]. We have previously cloned the short form of DPP10 ($DPP10_{789}$) from human brain [27]. To further characterise its function, we generated an antibody specific to $DPP10_{789}$ to examine the expression of $DPP10_{789}$ in human brains. Here we report that $DPP10_{789}$ is predominantly localized to neuronal soma and dendrites in the neocortex and subcortical grey matter in control brains and abnormally accumulated in Alzheimer's disease and other diseases characterised by tau positive pathologies.

## 2. Materials and Methods

*2.1. Primary Antibodies.* The peptide H-MRKVESRGEGGRE-OH containing the $N$-terminus of $DPP10_{789}$ was ordered from MIMOTOPES (VIC, Australia). This $N$-terminal sequence shares no sequence identity with the two other forms of DPP10 or the $N$-termini of the four DPP6 isoforms and therefore will only detect the $DPP10_{789}$ isoform of DPP10 [29]. Rabbits were immunised by the peptide mixed with Freund's complete adjuvant. $DPP10_{789}$ antiserum was purified using an affinity column prepared from the respective immunising peptide (ABGENT, Inc., San Diego, CA, USA) conjugated to 6% cross-linked beaded agarose. A sequence homology search was performed using BlastP into the GenBank database and the peptide sequence only had significant homology with $DPP10_{789}$. All other primary antibodies, their source, and the dilution used in the present studies are listed in Table 1.

*2.2. Human Cases.* Samples from the hippocampus, the frontal and temporal cerebral cortex, the entorhinal and cingulated cortex, and the cerebellum were obtained from individuals listed in Table 2. Brain tissue was collected by the National Health Medical Research Council (NHMRC) Brain Bank of South Australia following NHMRC ethical guidelines. All diseased cases had a clinical diagnosis while control cases showed no clinical signs of dementia.

*2.3. Cell Culture and Sample Preparation.* The human kidney epithelial cell line 293T was cultured as described previously [30]. Transfection with GFP-$DPP10_{789}$ construct was carried out by methods previously described using Fugene 6 (Roche, USA) [27, 30]. After 48 hrs, cell extracts were resuspended in

Table 2: Human cases analysed in this study.

| Brain Bank number | Gender | Age | Postmortem delay (h) | Neuropathological diagnosis |
|---|---|---|---|---|
| SA0123 | M | 80 | 21 | AD |
| SA0126 | F | 79 | 31 | AD |
| SA0134 | F | 69 | 23 | AD |
| SA0143 | M | 84 | 15 | AD |
| SA0148 | M | 81 | 14 | AD |
| SA0129 | F | 88 | 9 | Early AD |
| SA0087 | M | 71 | 15.5 | FTLD |
| SA0069 | M | 69 | 31 | DLBD |
| SA0079 | F | 82 | 31 | DLBD |
| SA0063 | F | 81 | 7 | DLBD |
| SA0094 | M | 74 | 24 | DLBD |
| SA0035 | F | 72 | 28 | PSP |
| SA0043 | F | 69 | 10 | PSP |
| SA0106 | M | 66 | 29 | PSP |
| SA0136 | F | 80 | 20 | PSP |
| SA0010 | M | 58 | 14 | Control |
| SA0013 | M | 64 | 23 | Control |
| SA0021 | F | 72 | 7 | Control |
| SA0030 | M | 69 | 48 | Control |
| SA0031 | F | 61 | 8 | Control |

AD: Alzheimer's disease, DLBD: diffuse Lewy's body disease, FTLD: frontotemporal lobar degeneration, PSP: progressive supranuclear palsy, F: female, and M: male.

sonication buffer (20 mM Tris pH 7.5, 5 mM EGTA, 2 mM EDTA and 0.25 M sucrose) and sonicated for 3 × 10 sec. Following sonication cellular debris was removed by a brief 10,000 g centrifugation and then the supernatant underwent a 30 min 100,000 g centrifugation at 4°C to pellet membrane proteins. The membrane pellet was solubilized in sonication buffer containing 0.5% Triton X-100, mixed with 4x sample buffer (6% SDS, 40% sucrose, 150 mM Tris pH 6.8, and 0.03% Bromophenol Blue), and incubated at 37°C for 10 mins and run on 10% SDS-PAGE. The recombinant GFP-tagged $DPP10_{789}$ protein was detected using either an anti-GFP antibody (Cell Signaling Technology, USA) or the affinity purified anti-$DPP10_{789}$ antibody described above.

*2.4. Tissue Preparation.* Brain tissues were fixed routinely by immersion in a mixture of 4% paraformaldehyde and picric acid. Series of each frozen section (450 $\mu$m thick) were cut on a chilled microtome. Paraffin sections were cut (5–20 $\mu$m), mounted on gelatine coated glass slides, and dried in an oven at 37°C overnight.

*2.5. Immunohistochemistry.* A green fluorescent protein GFP-$DPP10_{789}$ construct with GFP fused to the *N*-terminus of $DPP10_{789}$ was transiently transfected into 293T cells cultured on a chamber slide as described previously [27]. After 48 h, cells were washed with PBS and then fixed with 2% paraformaldehyde made in PBS. The affinity purified anti-$DPP10_{789}$ Ab was used to detect recombinant $DPP10_{789}$ protein. Mouse anti-rabbit Alexa 596 (Molecular Probes, Eugene, OR) was used as the secondary antibody for immunofluorescence studies.

Free-floating sections of human brain (50 $\mu$m) were incubated with primary antibody for 48 h at 4°C. Incubation with the secondary biotinylated anti-rabbit or anti-mouse IgG was performed for 1 hr at room temperature. Immunoreactions were visualised with the avidin-biotin-peroxidase complex (VECTASTAIN ABC system, Vector Labs, UK) and 3-3-diaminobenzidine-4 $HCl/H_2O_2$ (DAB, D5637 Sigma, USA). Paraffin-embedded sections were treated similarly after dewaxing, except that they were heat-treated (105°C for 10 min 1 mM EDTA, pH 8.0 at 25°C) before immunostaining.

Double-labelled immunohistochemistry was performed on sections from AD cases. Selected free-floating sections were incubated with both anti-$DPP10_{789}$ and AT8 antibody (anti-phosphorylated tau protein), Tau2 antibody (detects both phosphorylated and nonphosphorylated tau), or A4 antibody (anti-amyloid-$\beta$). Anti-$DPP10_{789}$ antibody was then visualized by anti-rabbit IgG conjugated with Cy2 (Jackson ImmunoResearch Laboratories Inc., USA) while anti-tau antibody or anti-amyloid antibody was detected by anti-mouse IgG conjugated with Cy3 (Jackson ImmunoResearch Laboratories).

Whenever the A4 antibody was used, antigen retrieval was performed before the blocking step by incubating the sections in preheated sodium citrate buffer (10 mM, pH 8.5) at 80°C for 30 min.

*2.6. Quantification of Lesions.* Adjacent free-floating sections of hippocampus or cortex were immunostained with $DPP10_{789}$, AT8, or A4 antibody separately using the DAB reaction as described above. The number of lesions was quantified at 200 times of magnification under an Olympus BH-2 light microscope (Tokyo, Japan) coupled to a MicroPublisher 3.3 RTV digital camera (QIMAGING, Canada). In the hippocampus, three fields (0.01 $mm^2$/field) from each region of Ammon's horn (CA1-4) were counted. In neocortical sections, three fields per case were counted in each of layers III to V. After each field was captured, the stage was moved manually to a new field using fiducial landmarks to ensure a completely nonredundant evaluation.

*2.7. Tissue Homogenates.* Hippocampuses of five AD cases and four control cases were dissected from fresh-frozen brain. Samples were homogenized in 10 volumes of ice-cold sucrose buffer (0.32 M sucrose, 1 mM EDTA, 5 mM Tris-HCl, and pH 7.4) containing 0.2% Triton X-100 and a protease inhibitor cocktail (Sigma, USA). The homogenate was centrifuged at 10,000 ×g for 20 min. The supernatant was saved and the pellet was then resuspended in ice-cold sucrose buffer and homogenized again. The homogenate was solubilised for 1 hr at 4°C. Insoluble material was removed by centrifugation at 10,000 ×g for 30 min. The second supernatant was combined with the first as hippocampal solubilised fraction. After the estimation of protein concentration, aliquots of homogenates were immediately subjected to incubation with 4 × SDS-PAGE sample buffer (250 mM Tris-HCl, 8% SDS, 40% glycerol, 0.4 M DTT, 0.04% Bromophenol Blue, and pH 6.8) at 37°C for 20 min. Protein (50 $\mu$g) from each sample was loaded and run on a 10% SDS-PAGE gel.

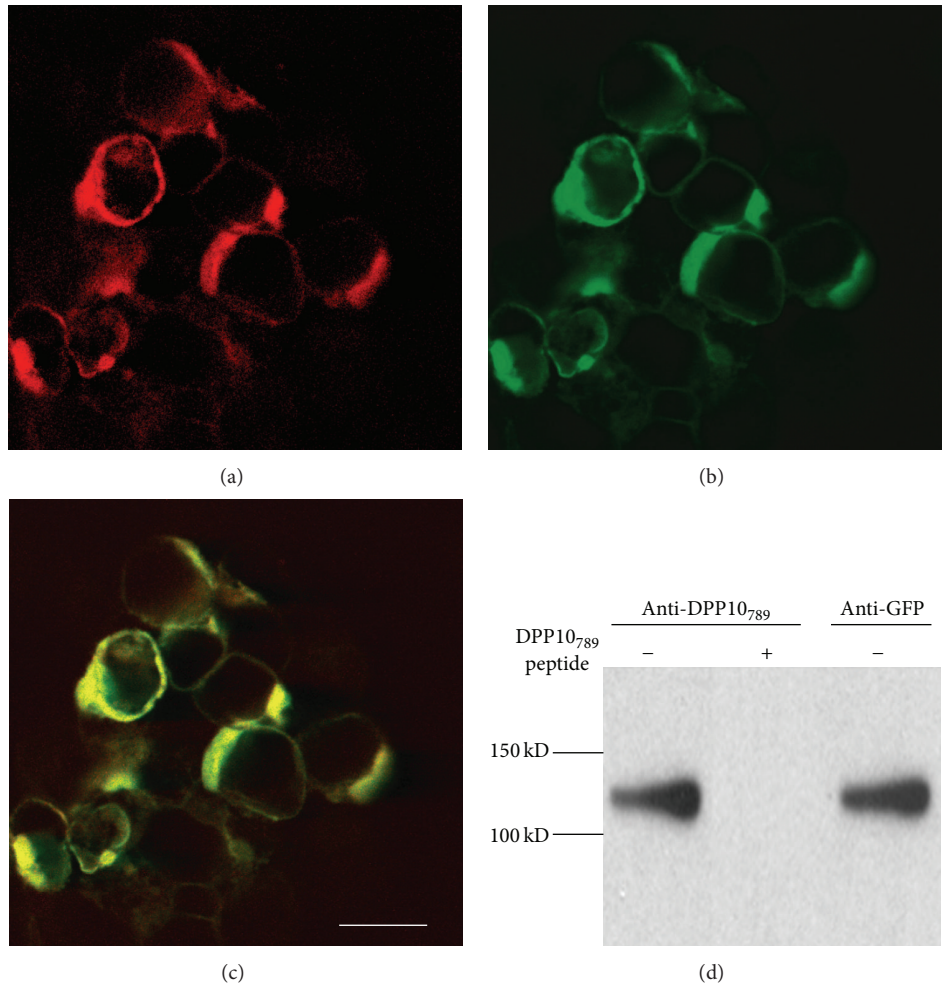


FIGURE 1: Anti-DPP10$_{789}$ antibody characterization. The GFP-DPP10$_{789}$ construct was transiently transfected into 293T cells. DPP10$_{789}$ protein was stained with anti-DPP10$_{789}$ antibody followed by Cy3 goat anti-rabbit IgG (a). The green GFP fluorescence (b) and the overlay of the Cy3 and the GFP images (c). Scale bar is 20 $\mu$m. Membrane fractions were prepared and run on a 10% SDS-PAGE gel. The transferred membrane was immunoblotted with DPP10$_{789}$ antibody. The DPP10$_{789}$ antibody recognized a 120 kDa band corresponding to the full-length GFP-tagged DPP10$_{789}$ ((d) far left lane). This 120 kDa band can be totally blocked with addition of the antigenic peptide for DPP10$_{789}$ antibody in the blocking solution ((d) middle lane). The anti-GFP antibody detected the same band after the membrane was stripped and reprobed ((d) right lane).

*2.8. Immunoblot.* Immunoblots were performed as described previously [27] and incubated with the affinity purified DPP10$_{789}$ antibody (final concentration at 1.25 $\mu$g/mL) or anti-$\beta$III-tubulin monoclonal antibody (final concentration 0.1 $\mu$g/mL) at 4°C overnight. Bound antibodies were detected using the SuperSignal West Pico Chemiluminescent Substrate (Pierce, IL, USA). The membrane was exposed to X-OMAT diagnostic film (Kodak Scientific Light Systems, NY, USA) and developed on a Kodak X-OMAT 1000 Processor (Kodak Australasia, Pty. Ltd.).

*2.9. Analytical Methods.* The protein concentrations of brain homogenates were measured using the Bradford assay (Bio-Rad, USA) according to the manufacturer's instructions. Levels of DPP10$_{789}$ in brain homogenates were estimated by immunoblot using the Quantity One (BioRad, USA) image analysis software package and were adjusted by the level of neuron specific protein $\beta$-tubulin. An independent $t$-test was performed to compare the expression of DPP10$_{789}$ between control and AD brains.

## 3. Results

*3.1. Specificity of the DPP10$_{789}$ Antibody.* To confirm the specificity of the anti-DPP10$_{789}$ antibody, we used immunofluorescence and immunoblots to examine the 293T cells transfected with the GFP-DPP10$_{789}$ construct (Figures 1(a)–1(d)). With immunofluorescence, all cells that expressed GFP fluorescence were detected by the anti-DPP10$_{789}$ antibody (Figures 1(a), 1(b), and 1(c)), indicating the antibody specifically bound to recombinant GFP-DPP10$_{789}$ chimeric protein. Our DPP10$_{789}$ antibody was designed to detect the $N$-terminal sequence of DPP10$_{789}$, while the anti-GFP antibody recognises the GFP protein. On immunoblot (Figure 1(d)), the DPP10$_{789}$ antibody recognised a band around 120 kDa (Figure 1(d), far left lane), corresponding to the expected

molecular mass of GFP-tagged DPP10$_{789}$ and being consistent with our previous studies [27]. The 120 kDa band was also detected by the anti-GFP antibody (Figure 1(d), right lane) confirming that the band was the GFP-DPP10$_{789}$ chimeric protein. Because 293T cells are derived from human kidney epithelial cells that do not express the brain derived DPP10$_{789}$, no endogenous DPP10$_{789}$was detected by immunoblot. Thus these results confirmed that the DPP10$_{789}$ antibody was specific to DPP10$_{789}$.

*3.2. DPP10$_{789}$ in Control and AD Brains.* To document the cellular localisation of DPP10$_{789}$ protein in human brains, we first immunostained free-floating brain sections from a selection of control cases and cases with various neurodegenerative diseases (Table 2). In control brains, positive DPP10$_{789}$ staining was predominantly associated with neurons in the CA1 region of the hippocampus (Figures 2(a), 3(a), and 3(b)). The pyramidal cells were particularly well stained, with DPP10$_{789}$ reactivity extending well into the distal portion of dendrites (Figures 3(a) and 3(b)).

In contrast, very strong punctate DPP10$_{789}$ immunoreactivity was observed in AD brains especially in the hippocampal regions. Close examination revealed that neurofibrillary tangles and dystrophic neurites were robustly stained with the DPP10$_{789}$ antibody. These positive structures were most abundant in the hippocampal region, where staining was most intense in the CA1 and subiculum areas (Figures 2(b)–2(e) and 2(h)). This immunoreactivity was completely abolished by the DPP10$_{789}$ antigenic peptide (Figure 2(i)), and sections incubated with preimmunization serum omitting the DPP10$_{789}$ antibody did not show any positive staining (data not shown), further indicating that the observed immunostaining was specific.

At high magnifications, three types of DPP10$_{789}$ positive neurofibrillary tangle-like structures were observed: (1) granular staining in the neuronal soma (Figure 2(j)), resembling pretangle phosphotau aggregates; (2) condensed intraneuronal staining (Figures 2(k), 2(l), and 2(o)), resembling intraneuronal tau NFTs; (3) less condensed extracellular staining (Figures 2(m), 2(n), and 5(h)), resembling extraneuronal tau NFTs and ghost tangles. In addition, DPP10$_{789}$ immunoreactivity was also detected significantly in dystrophic neurites surrounding amyloid plaques (Figures 2(d), 2(e), arrows, and 2(p)) and in neuropil threads (Figure 2(q)).

The DPP10$_{789}$ positive tangles and dystrophic neurites were also observed in the frontal, temporal, entorhinal, and cingulate regions as summarized in Table 3. No DPP10$_{789}$ positive staining was observed in the cerebellum.

Similar results were also observed in paraffin-embedded sections. DPP10$_{789}$ immunostaining was detected on the cell body and surface of dendrites of the hippocampal region in a control case (Figures 3(a), arrows, and 3(b)). DPP10$_{789}$ positive staining was also observed in NFTs and plaque-associated dystrophic neurites in AD brain (Figures 3(c)–3(h)). Thus the above results suggested that the increased DPP10$_{789}$staining was primarily accumulated in neurofibrillary tangles and dystrophic neurites.

*3.3. DPP10$_{789}$ in Other Tauopathies.* Because neurofibrillary tangle and dystrophic neurite pathologies also occur in neurodegenerative diseases other than AD, including PSP and FTLD and DLBD, these later cases were further examined. Some DPP10$_{789}$ positive tangles and plaques were also detected in these cases (Figure 4). Table 3 summarizes the presence of DPP10$_{789}$ positive tangles and dystrophic neurites. In the four DLBD cases examined, DPP10$_{789}$ positive tangles and dystrophic neurites were also observed in temporal, hippocampal, and entorhinal cortex regions (Figures 4(b) and 4(e)). A few positive DPP10$_{789}$ tangles and plaques in the hippocampal and entorhinal regions were observed in PSP cases (Figure 4(c)). Occasionally weak DPP10$_{789}$ positive tangles and plaques were detected in some aged control brains.

*3.4. DPP10$_{789}$ Colocalizes with Tau Protein but Not with Amyloid-$\beta$ in AD Brain.* Because tau protein is a major component of neurofibrillary tangles and dystrophic neurites, we examined if DPP10$_{789}$ protein expression is associated with tau protein expression. We used the DPP10$_{789}$ antibody and anti-tau antibody (AT8) specific for phospho-Ser202/Thr-205 to localise DPP10$_{789}$ and phosphorylated tau (p-tau) by double immunofluorescence staining in the brains of AD. We observed robust colocalization of DPP10$_{789}$ with p-tau in most tangles and dystrophic neurites (Figure 5). In neurofibrillary tangles, DPP10$_{789}$ and p-tau were fully colocalized (Figures 5(b), 5(e), and 5(g)). In plaques, DPP10$_{789}$ and p-tau were found in the larger sized dystrophic neurites (Figure 5(d)). DPP10$_{789}$ was also present in intracellular vesicle-like structures (Figure 5(f)) where only weak p-tau staining was present. In the entorhinal region of the temporal cortex, some DPP10$_{789}$ positive tangle-like structures were devoid of p-tau staining (Figure 5(h)), indicating that the DPP10$_{789}$ antibody might be able to detect either early or late tangle stages—ghost tangles which are not detected by AT8. Double staining using the DPP10$_{789}$ antibody and Tau2 antibody (detects both phosphorylated and nonphosphorylated tau) also showed colocalization of DPP10$_{789}$ and tau in neurofibrillary tangles and dystrophic neurites (Figures 5(a) and 5(c)).

The other major pathological hallmark of AD is the neuritic amyloid plaques located in the extracellular space of the brain, comprised of an aggregated A$\beta$ peptide core surrounded by dystrophic neurites. As the DPP10$_{789}$ antibody showed strong immunoreactivity in plaque-associated dystrophic neurites, it was also examined if DPP10$_{789}$ colocalized with A$\beta$ peptide. Double immunofluorescence revealed that DPP10$_{789}$ positive dystrophic neurites were mostly present in the A$\beta$ core of senile plaques. While both DPP10$_{789}$ and A$\beta$ positive staining were observed within the same plaque region, they were not colocalized; the red A$\beta$ staining was distributed as amyloid aggregation, with the green DPP10$_{789}$ positive dystrophic neurites mingling randomly (Figure 5(i)).

The intrahippocampal distribution of DPP10$_{789}$ positive neurofibrillary tangles (NFTs) followed the pattern established for p-tau positive ones, with the greatest number of involved neurons lying within the CA1 region of Ammon's

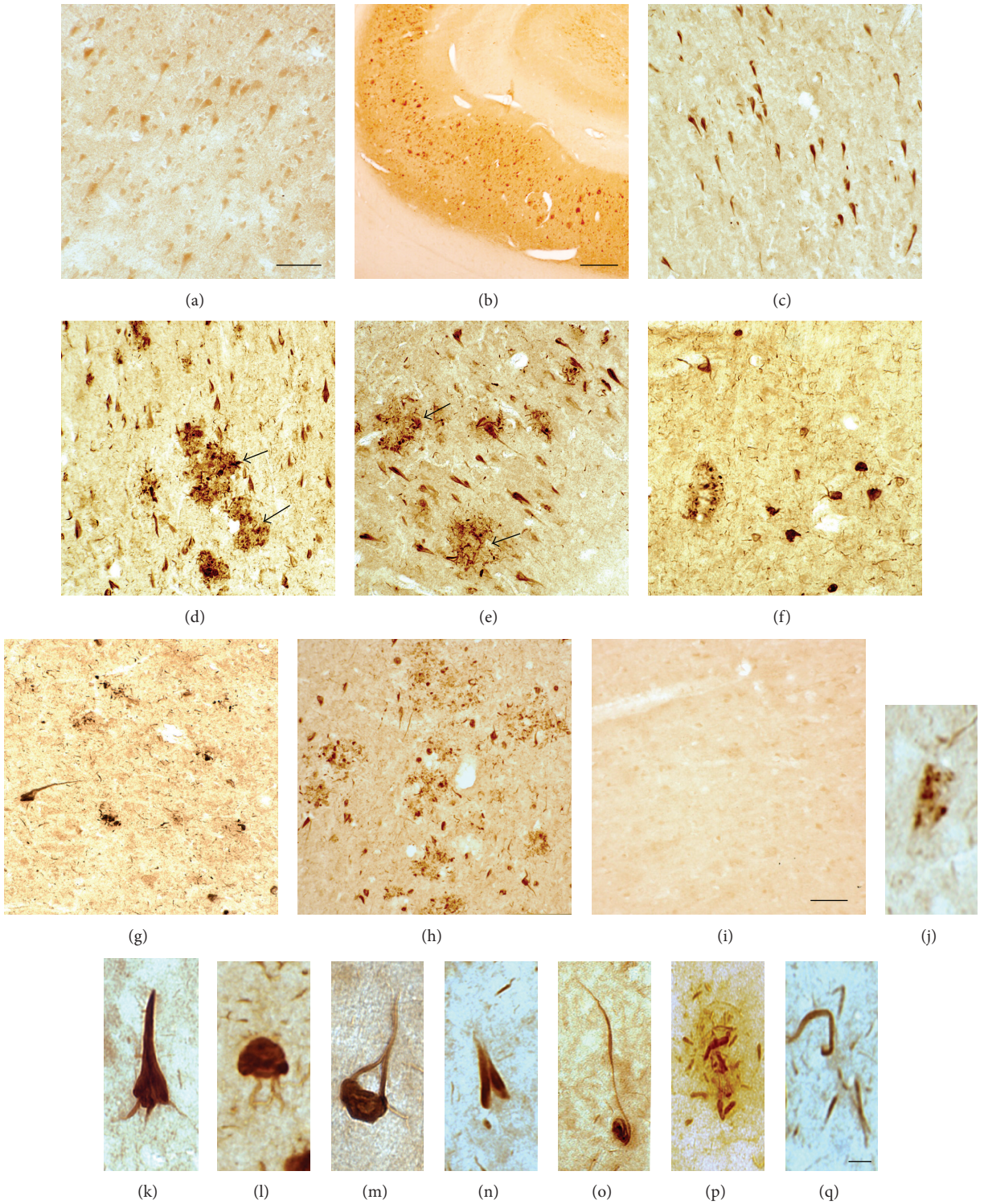


FIGURE 2: Immunostaining of $DPP10_{789}$ in free-floating sections of control and AD brains. $DPP10_{789}$ immunostaining in the CA1 region of a control brain (a), CA1 and subiculum region (b, c, and d), CA2 (e), inferior frontal cortex (f), cingulated cortex (g), inferior temporal cortex (h), and inferior temporal cortex section blocked with antigenic peptide (i) in AD brains. $DPP10_{789}$ staining was found in granular structures in the neuronal soma (j), NFT with extensions into dendrites of pyramidal neurons (k), globose NFT (l), extracellular ghost tangle (m), flame shaped NFT (n), slender tangle of the subiculum with long extension into apical dendrite (o), plaque-associated dystrophic neurites (p), and neuropil threads (q). Scale bar is 200 $\mu$m (b), 50 $\mu$m (a, c–i), and 10 $\mu$m (j–q). Arrows in (d) and (e) indicate staining in plaque-associated dystrophic neurites in AD brain.

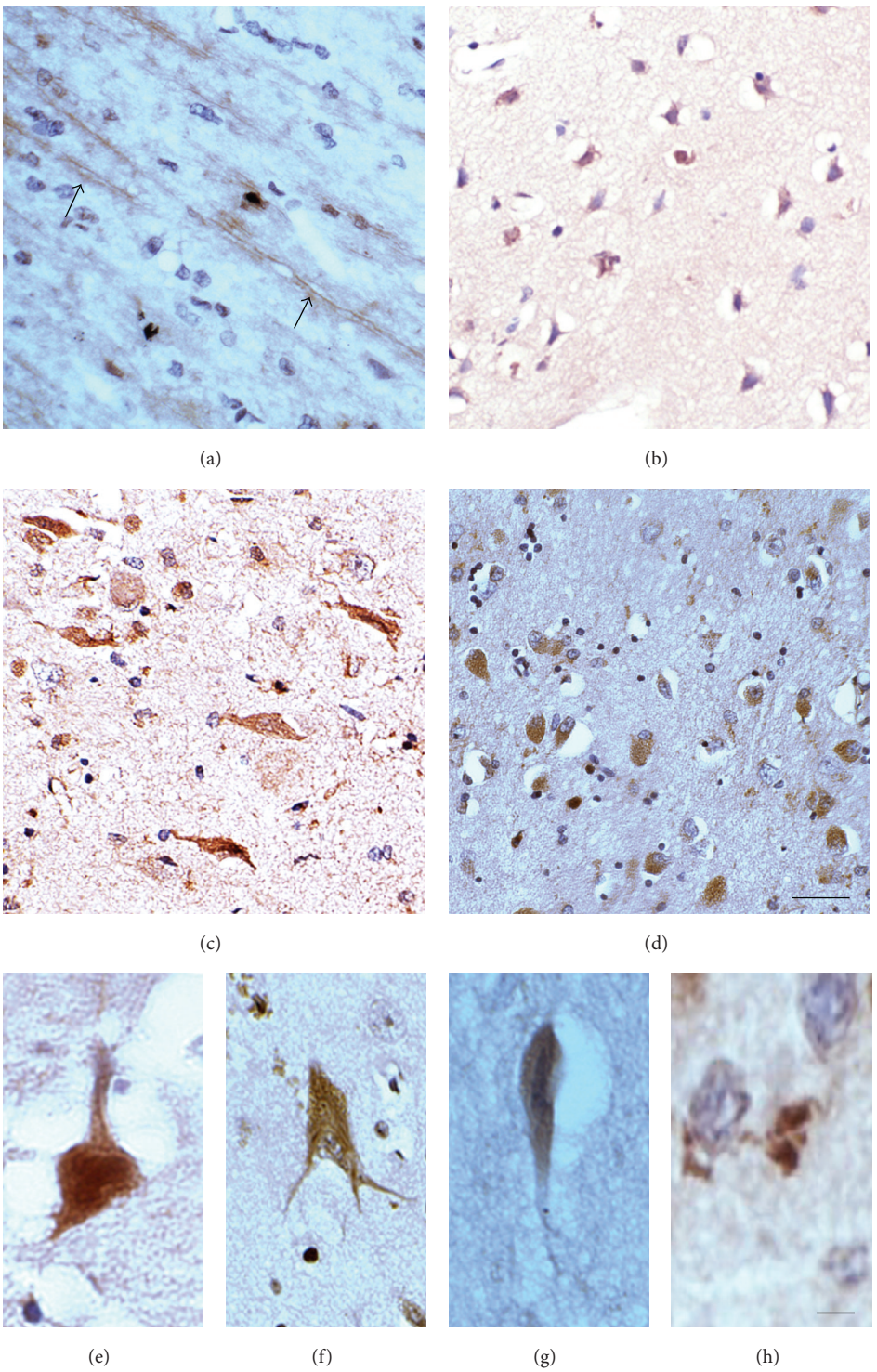


FIGURE 3: Immunostaining of $DPP10_{789}$ in paraffin sections from control and AD brains. $DPP10_{789}$ reactivity was observed in the frontal cortex of a control individual (a, b), and arrows indicate the surface staining of $DPP10_{789}$ in dendrites. $DPP10_{789}$ positive staining was increased in AD brain (c, d) and in NFTs (e–h). Scale bar is 50 $\mu$m (a–d) and 10 $\mu$m (e–h).

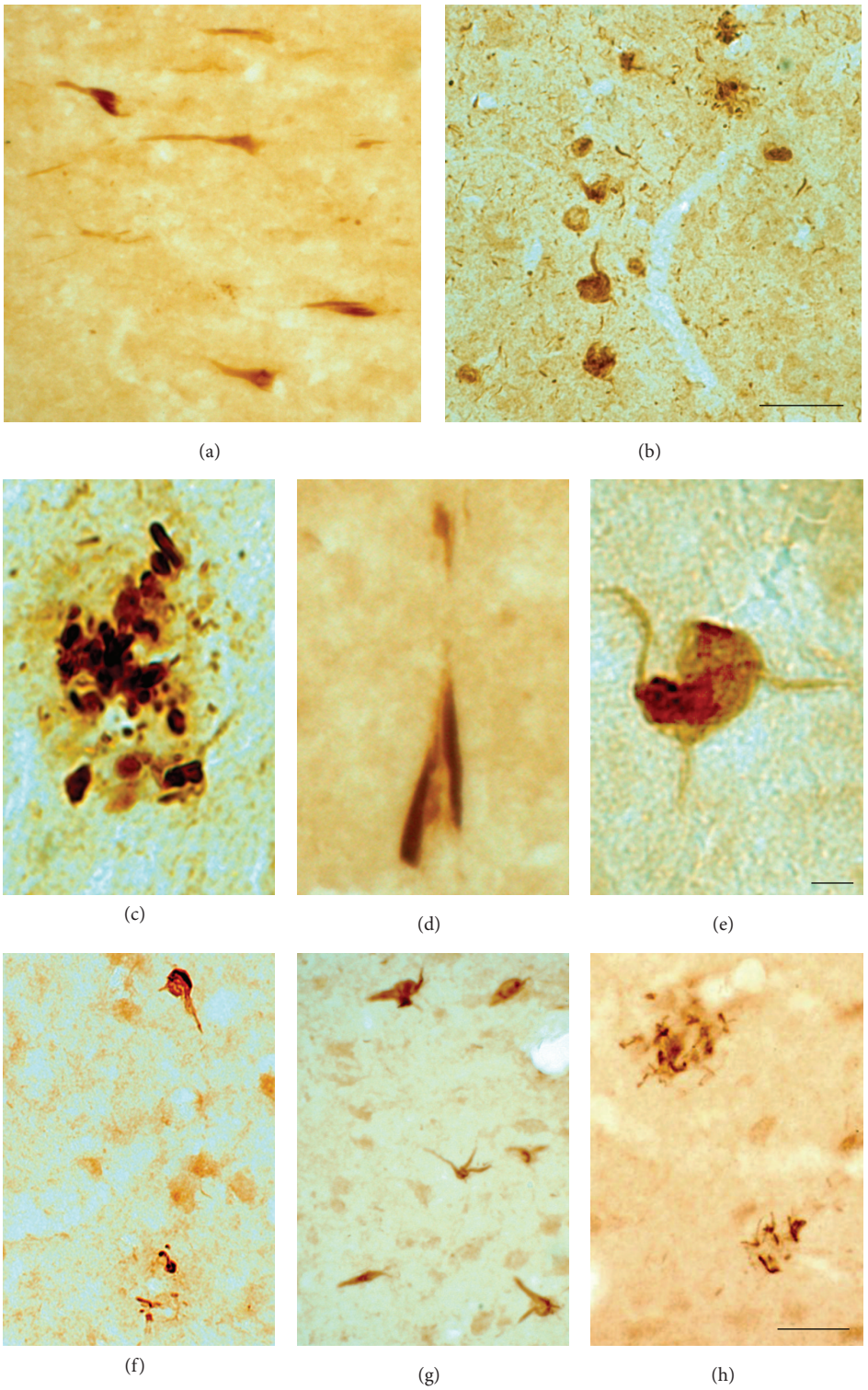


FIGURE 4: $DPP10_{789}$ immunostaining in free-floating brain sections of other tauopathies. $DPP10_{789}$ positive NFTs were observed in the hippocampus of FTLD (a, d and g) and PSP (f) and superior frontal brains sections from patients with DLBD (b, e). $DPP10_{789}$ staining in plaque-associated dystrophic neurites in DLBD and PSP brains (c and h, resp.). Scale bar is 50 $\mu$m (a, b, and f–h) and 10 $\mu$m (c–e).

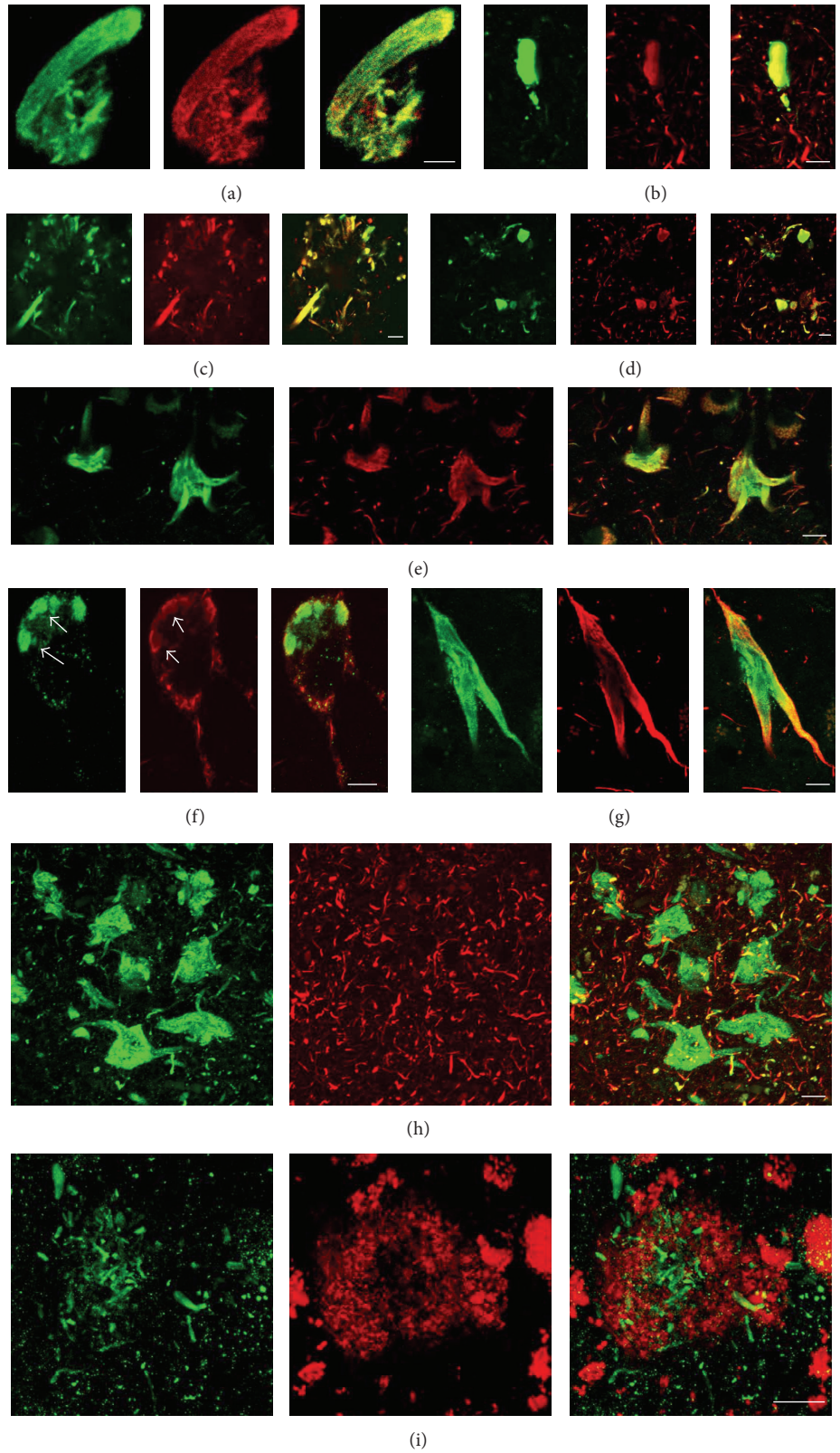


FIGURE 5: $DPP10_{789}$ and tau colocalization in AD. Immunohistochemical colocalization of $DPP10_{789}$ with phosphorylated tau (p-tau) in tangles and plaque-associated dystrophic neurites. $DPP10_{789}$ (green) partially or fully colocalized with p-tau (red) in tangles (a, b, e, and g) and in plaque-associated dystrophic neurites (c, d). $DPP10_{789}$ was also present in intracellular vesicle-like structures (f) where very weak staining for p-tau was present. $DPP10_{789}$ immunoreactivity was also found in some tangles in the entorhinal region which were devoid of p-tau staining (h). $DPP10_{789}$ (green) did not colocalize with amyloid-$\beta$ plaques (red) in AD brain (i). Scale bar is 10 $\mu$m. (a) and (c) used Tau2 ab and the remaining images are with AT8 ab.

Table 3: Summary of the $DPP10_{789}$ positive staining in NFT and plaque-associated dystrophic neurites observed in control and neurodegenerative disease cases.

| | Case number | Neuropathological diagnosis | Frontal cortex | | Temporal cortex | | Hippocampus | | Entorhinal cortex | | Cingulate cortex | |
|---|---|---|---|---|---|---|---|---|---|---|---|---|
| | | | Tangle | Plaque | Tangle | Plaque | Tangle | Plaque | Tangle | Plaque | Tangle | Plaque |
| 1 | SA0123 | AD | − | +++ | +++ | +++ | +++ | +++ | +++ | +++ | ++ | +++ |
| 2 | SA0126 | AD | +++ | ++ | +++ | +++ | ++ | +++ | +++ | ++ | ++ | ++ |
| 3 | SA0134 | AD | + | +++ | − | +++ | +++ | ++ | N/A | N/A | + | +++ |
| 4 | SA0143 | AD | + | + | +++ | ++ | +++ | +++ | +++ | +++ | + | + |
| 5 | SA0148 | AD | +++ | +++ | − | +++ | +++ | +++ | +++ | +++ | +++ | +++ |
| 6 | SA0129 | Early AD | + | + | + | + | +++ | ++ | +++ | + | − | − |
| 7 | SA0069 | DLBD | ++ | ++ | − | +++ | ++ | ++ | +++ | +++ | + | ++ |
| 8 | SA0079 | DLBD | − | − | − | − | − | ++ | − | − | − | − |
| 9 | SA0094 | DLBD | − | − | +++ | +++ | + | ++ | ++ | ++ | + | + |
| 10 | SA0063 | DLBD | − | − | + | − | + | + | − | − | − | − |
| 11 | SA0087 | FTLD | − | − | − | − | +++ | + | ++ | − | − | − |
| 12 | SA0035 | PSP | − | − | + | − | + | − | N/A | N/A | − | − |
| 13 | SA0043 | PSP | + | + | + | + | ++ | + | ++ | ++ | + | − |
| 14 | SA0106 | PSP | − | − | − | − | − | − | ++ | N/A | − | − |
| 15 | SA0136 | PSP | − | − | − | + | − | ++ | +++ | + | − | − |
| 16 | SA0010 | Control | + | − | − | + | − | − | − | − | − | + |
| 17 | SA0013 | Control | − | − | − | − | + | − | − | − | − | − |
| 18 | SA0021 | Control | − | − | − | − | + | − | + | − | − | − |
| 19 | SA0030 | Control | − | − | + | − | − | − | N/A | N/A | + | + |
| 20 | SA0031 | Control | − | − | − | − | N/A | N/A | N/A | N/A | − | − |

The number of lessons was counted at ×200 magnification under an Olympus BH-2 light microscope (Tokyo, Japan).
N/A: sample not available; −: negative; +: 1–5 lesions/field; ++: 5–10 lesions/field; +++: >10 lesions/field.

horn, followed by CA2, CA3, and CA4 (Figure 6(a)). In the neocortical region, staining was detected mainly in layers III–V. Approximately 67% of p-tau positive NTFs and 40% A$\beta$ positive neuritic plaques (NPs) contained anti-$DPP10_{789}$ immunoreactivity in these regions (Figure 6(b)).

*3.5. Truncated $DPP10_{789}$ Is Elevated in AD Tissue.* $DPP10_{789}$ protein levels were analyzed in the hippocampus as it is a rich source of both NFTs and NPs. The $DPP10_{789}$ Ab detected three major mobilities: 100 kDa, 50 kDa, and 37 kDa (Figure 7(a)) in immunoblots. The 100 kDa band represents the full-length $DPP10_{789}$ protein [27]. Samples from both AD and control brains showed similar density of this band. The 50 kDa and 37 kDa bands observed are probably truncated forms of $DPP10_{789}$ which are less than half the size of intact $DPP10_{789}$ and have retained the $N$-terminus, suggesting that the $DPP10_{789}$ has been proteolytically processed. Noticeably, AD brain samples had higher density bands of these two truncated forms compared to control samples. Quantitation of the immunoblot normalised to tubulin immunoreactivity confirmed that there was no significant difference in the 100 kDa intensity band between AD and control brains. However, the immunoreactive intensity of 50 kDa, 37 kDa, and 50 + 37 kDa was all significantly elevated in AD brain compared to control brain ($P \leq 0.05\%$.) (Figure 7(b)), indicating the possibility that $C$-terminal truncated $DPP10_{789}$ may be aggregating and thus may be directly involved in the formation of neurofibrillary tangles and dystrophic neurites in AD brain.

## 4. Discussion

$DPP10_{789}$ is a dipeptidyl peptidase-like protein that together with Kv-channel interacting proteins (KChIPs) forms multiprotein complexes that underlie subthreshold A-type currents ($I_{SA}$) in neuronal somatodendritic compartments [28]. This is the first study to assess the expression of $DPP10_{789}$ in postmortem brain samples in AD and other major tauopathies. Using immunohistochemistry we reveal predominant neuronal staining of $DPP10_{789}$ throughout the neocortex and subcortical grey matters with high expression in the pyramidal cells in control brain tissue. In contrast, in AD brains, robust $DPP10_{789}$ reactivity was also detected in neurofibrillary tangles and plaque-associated dystrophic neurites, most of which colocalized with the hyperphosphorylated Ser-202/Thr-205 tau epitope. $DPP10_{789}$ positive neurofibrillary tangles and plaque-associated dystrophic neurites also appeared in other neurodegenerative diseases such as FTLD, DBLB, and PSP. Occasional $DPP10_{789}$ positive neurofibrillary tangles and neurites were seen in some aged control brains. Furthermore using a quantitative analysis we showed that truncated $DPP10_{789}$ fragments increased significantly in AD brains compared to control brains. These results provide the

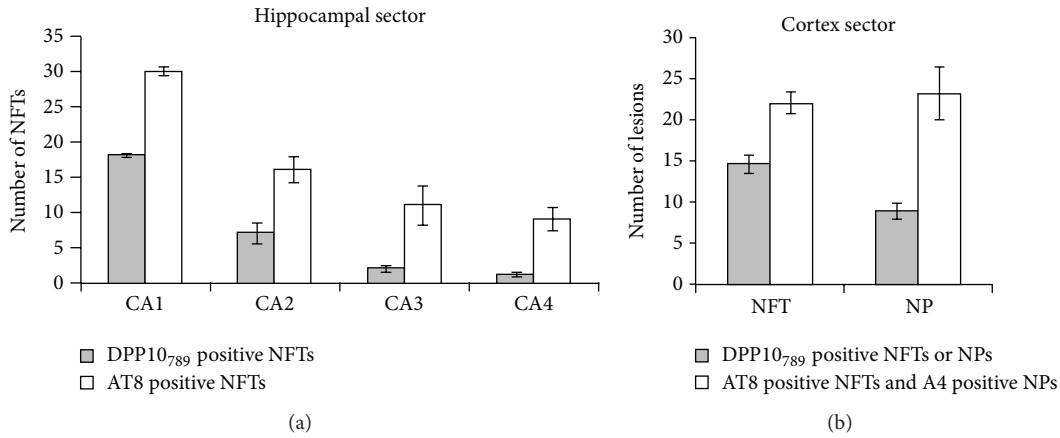


FIGURE 6: The regional distribution of $DPP10_{789}$ positive NFTs and NPs compared with phosphotau positive NFTs and amyloid-$\beta$ positive plaques. The adjacent free-floating sections of hippocampus or cortex were immunostained with $DPP10_{789}$, AT8, or A4 antibody separately using the DAB reaction. (a) The distribution patterns of $DPP10_{789}$ positive NFTs and tau positive NFTs in AD hippocampal sector. Three fields (0.01 $mm^2$/field) per case from each region of Ammon's horn (CA1-4) were counted. (b) In the cortex sector of AD brain, the number of $DPP10_{789}$ positive NFTs and NPs was compared with tau positive NFTs and amyloid-$\beta$ positive NPs. Three fields (0.01 $mm^2$/field) per case were counted in each of layers III to V. Bars reflect mean ± SE ($n = 9$; observations from 3 fields/case × 3 cases).

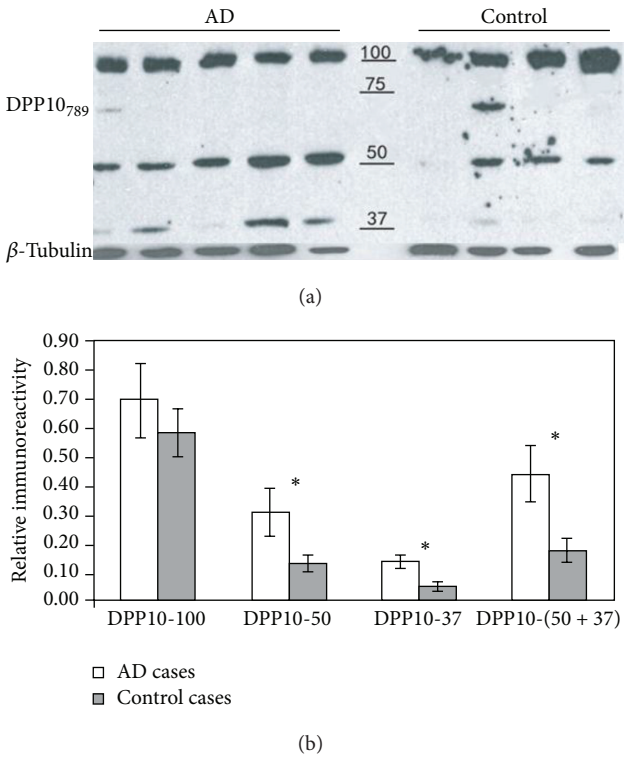


FIGURE 7: Truncated $N$-terminal $DPP10_{789}$ levels were elevated in AD hippocampus relative to control hippocampus. 50 $\mu$g of solubilised fractions prepared from fresh-frozen AD and control hippocampus was subjected to immunoblot analysis with $DPP10_{789}$ antibody and class III $\beta$-tubulin antibody (a). Quantification of immunoblot data (b). The value of $y$-axis represents the relative immunoreactivity normalised to tubulin expression level. Bars represented mean ± SE of duplicate determination from five AD and four control hippocampal homogenates. "*" represented one-tailed $t$-test $P \leq 0.05\%$.

first evidence that $DPP10_{789}$ may be involved in the pathology of AD and other neurodegenerative diseases.

Our immunohistochemistry studies revealed that in control brains $DPP10_{789}$ immunoreactivity is located in the cell body of neurons throughout the grey matter of cerebral cortex and axonal fibre tracts of white matter (Figures 2(a) and 3(a)), suggesting that $DPP10_{789}$ protein is widely distributed in the neuronal cells which is consistent with the expression of DPP10 mRNA reported in rat brain [28]. In human there are potentially four DPP10 mRNA isoforms which all have unique amino acid sequences in the $N$-terminal intracellular domain but identical $C$-terminal extracellular domains [31]. Multiple DPP10 isoforms have been observed by both Northern blot and reverse transcriptase PCR in both human brain and pancreas; however it is not known which transcript on the Northern blot represents $DPP10_{789}$ or whether any of these mRNA isoforms are translated into different forms of DPP10 protein *in vivo* [27, 31–33]. Takimoto et al. demonstrated the presence of four DPP10 mRNA isoforms in human brain. These isoforms are different only at the $N$-terminal amino acid sequence. When the different $N$-terminal forms of DPP10 were co-expressed with the Kv4.3 channel there were no differences in the gating ability of the channel [31]. In their study DPPYd is equivalent to $DPP10_{789}$ and this form was also detected in rat brain. Interestingly Takimoto et al. were unable to detect $DPP10_{796}$ in the adrenal gland and pancreas of humans or rats. In our laboratory we have found it extremely difficult to use reverse transcriptase PCR to amplify the other DPP10 isoforms (data not shown) from either postmortem brain tissue or neuronal cell lines; therefore these mRNA transcripts and thus protein isoforms appear to be present in very low amounts in human tissues.

Throughout the cortex of AD cases, although the background distribution pattern of $DPP10_{789}$ is similar to controls, it was the neurofibrillary tangles and plaque-associated

dystrophic neurites that, by virtue of their intense $DPP10_{789}$ staining, stand out compared to controls (some aged controls also had a few $DPP10_{789}$ tangles). Our data also revealed that the $DPP10_{789}$ positive tangles and plaque-associated dystrophic neurites are distributed mainly in layers III–V pyramidal cells of the neocortex and CA1 and CA2 pyramidal cells of the hippocampus in AD brains, consistent with the distribution of Kv4.2 and Kv4.3 subunits in brain [34]. DPP10 interacts with both Kv4.2 and Kv4.3 subunits [17, 35]. Additionally, Kv4 channels play important roles particularly in regulating neuronal membrane excitability; therefore these results indicate that deposition of $DPP10_{789}$ protein in these neurons may contribute to loss of channel function and lead to neuronal dysfunction and cell death in AD. Double immunofluorescence staining revealed that most of the $DPP10_{789}$ positive tangles were colocalized with the hyperphosphorylated phospho-Ser-202/Thr-205 tau epitope. In addition, the intrahippocampal distribution of $DPP10_{789}$ positive NFTs followed the pattern established for phospho-Ser-202/Thr-205 tau positive NFTs; however the amount of $DPP10_{789}$ positive NFTs was always less than that of phospho-Ser-202/Thr-205 tau (Figure 6(a)). This implies that, while AT8 can detect all six isoforms of human tau protein in brain [36], $DPP10_{789}$ may only be present in tangles containing a subset of the six isoforms. On the other hand, in the entorhinal cortex region, some $DPP10_{789}$ positive tangles were devoid of either AT8 (Figure 5(h)) or Tau2 (data not shown) antibody staining, indicating that $DPP10_{789}$ did not always cooccur with tau in tangles and it may on its own be involved with tangle formation without tau involvement. It is also possible that our $DPP10_{789}$ antibody can detect the late stage of tangles—the ghost tangles which have lost the phospho-Ser-202/Thr-205 tau epitope recognised by the AT8 antibody [37, 38]. Recently Lace et al. reported that the RD3 antibody that specifically recognises the 3-repeat tau shows an increased immunoreactivity in late-state ghost tangles [39]. Do RD3 positive tangles colocalize with $DPP10_{789}$ positive staining? Which tau isoform may be involved in $DPP10_{789}$ positive tangle formation? To answer these questions, further study needs to be done by using different tau antibodies specific to different tau isoforms.

Tau is a microtubule-associated protein and predominantly found in axons [40–42]. The best known functions of tau are the stabilization of microtubules and the regulation of axonal transport [43, 44]. Recently it was reported that tau has also been localized to dendrites under physiological conditions and at much lower levels [45]. In addition to its interaction with tubulin, tau binds to other partners such as the tyrosine protein kinase Fyn, dynactin, and postsynaptic density protein 95 (PSD95) [45–47]. Both tau-Fyn and tau-PSD95 interactions are involved in the complex formation of NMDA receptors with PSD95, which is required for excitotoxic downstream signalling, suggesting that the distribution of tau in dendrites is pivotal to healthy neurons [45, 47]. Noticeably, the intracellular distributions of Kv4 channels are also predominant in dendrites [34]. Besides, it has been reported that PSD95 has physical interactions with Kv4.2 [48, 49], suggesting that PSD95 may be involved in forming complexes between Kv4.2 and signalling molecules. Because the dendritic A-type potassium current strongly influences the induction of long-term potentiation also by NMDA receptors [50, 51], it is possible that there exist some signalling connections between tau, Fyn, PSD95, and Kv4. As a Kv4 channel associated protein, DPP10 also has the potential to be involved in these connections. However, so far there is no direct evidence showing that tau interacts with Kv4, and one possible explanation is that these protein interactions may be transient or unstable; thus it is difficult to detect the interactions using immunoprecipitation, immunostaining techniques, or other proteomic based methods.

$DPP10_{789}$ positive immunoreactivity was also observed in dystrophic neurites in A$\beta$ aggregated senile plaques. It was found that $DPP10_{789}$ positive dystrophic neurites did not colocalize but mingled with the A$\beta$ deposition core of the senile plaques. This is consistent with the fact that plaques are composed of extracellular aggregated A$\beta$, while $DPP10_{789}$, according to our studies, is distributed intracellularly or in the membrane [26, 27]. In addition, we have observed that the number of $DPP10_{789}$ positive neurofibrillary tangles and plaque-associated dystrophic neurites present in AD is much more than that observed in other tauopathies (Table 3). As the accumulation of A$\beta$ is a primary event driving AD pathogenesis, our finding indicates that $DPP10_{789}$ may be involved some way in the pathogenic process. So far, the mechanisms by which A$\beta$ mediates neurotoxicity and initiates the degenerative processes of AD are still not clear. Recent studies revealed that A$\beta$ inhibits the dendritic A-type K+ current in outside-out patches excised from distal dendrites of hippocampal CA1 pyramidal neurons, causing increases in back-propagating dendritic action-potential amplitude and associated $Ca^{2+}$ influx. These results suggest that the sustained increased dendritic $Ca^{2+}$ influx, which results from A$\beta$ deposition in dendritic arborisation that induces persistent inhibition of the A-type K+ current, may cause a loss of $Ca^{2+}$ homeostasis in dendrites of hippocampal neurons, an initiating event of synaptic failure and neurodegeneration [52]. Whether $DPP10_{789}$ is involved in this procedure needs further study.

The quantitative immunoblot on human brain samples showed that naturally *in vivo* two truncated forms of $DPP10_{789}$ are observed and the levels of these increase in AD brains compared to control brains, which has led us to hypothesise that the truncated forms may form aggregates in NFTs and dystrophic neurites. As there was no change in the full-length form of $DPP10_{789}$ between control and AD patients, it is assumed that if there is any increase in protein production in AD, the newly formed protein is likely to be rapidly degraded. $DPP10_{789}$ is a glycosylated transmembrane protein with a large extracellular *C*-terminal domain and a short intracellular *N*-terminal domain. The presence of $DPP10_{789}$ in NFTs and dystrophic neurites but not amyloid protein aggregated plaques suggests that $DPP10_{789}$ is confined to the neuronal cytoplasm. These observations suggest the possible aberrant trafficking of $DPP10_{789}$ in degenerating neurons.

DPP10 belongs to DPP4 gene family, some members of which have been reported to have multiple functions. Previous *in vitro* studies showed that DPP4 and FAP have roles in the cell-extracellular matrix interactions and apoptosis, and

these functions are independent of catalytic activity [53]. It is likely that most protein-protein interactions would occur on the $\beta$-propeller domains of these proteins [54]. With 47% amino acid similarity to DPP4, it is possible that DPP10, apart from associating with Kv4 channel complex through its single transmembrane domain [55], may also interact with other proteins and ligands via either its extracellular $\beta$-propeller domain or its intracellular domain and these interactions may control its biological function in normal and pathological conditions. Recently Lin et al. elegantly demonstrated that the highly related DPP6 interacts with filopodia-associated myosin and fibronectin within the extracellular matrix to play a role in hippocampal synaptic development [56]. In addition, DPP6 has been shown to interact with prion protein to mediate potassium channels and neuronal excitability [57].

In summary this paper reports the first evidence that $DPP10_{789}$ protein is present in NFTs and dystrophic neurites in AD. Interestingly, $DPP10_{789}$ protein colocalizes with hyperphosphorylated tau protein but not with A$\beta$. Moreover in neurodegenerative cases other than AD where neuronal tau pathology occurred, the same regions showed intense staining for $DPP10_{789}$. In addition this paper provides initial evidence that, as with other proteins involved in neurodegenerative diseases, $DPP10_{789}$ $C$-terminal truncation may lead to mistrafficking and aggregation of $DPP10_{789}$ protein but at this point it is unclear whether this occurrence contributes to AD pathology or is a result of AD pathology. Together this data suggests that DPP10 may play a significant role in the neurodegenerative process observed in AD and further investigation into this role and its interaction with tau is warranted.

## Abbreviations

| | |
|---|---|
| AD: | Alzheimer's disease |
| A$\beta$: | Amyloid-$\beta$ peptide |
| DAB: | 3-3-Diaminobenzidine-4 $HCl/H_2O_2$ |
| DLBD: | Diffuse Lewy's body disease |
| DP: | Dipeptidyl peptidase |
| FTLD: | Frontotemporal lobar degeneration |
| GFP: | Green fluorescent protein |
| Kv channel: | Voltage-gated potassium channel |
| KChIP: | Kv channel interacting protein |
| NFTs: | Neurofibrillary tangles |
| NPs: | Neuritic plaques |
| PSP: | Progressive supranuclear palsy. |

## Conflict of Interests

The authors declare that there is no conflict of interests regarding the publication of this paper.

## Authors' Contribution

Wei-Ping Gai and Catherine A. Abbott contributed equally to the paper. Tong Chen performed all experiments, data collection and analysis, and manuscript writing. Wei-Ping Gai and Catherine A. Abbott conceived the study, data interpretation, and manuscript writing.

## Acknowledgments

Dr. Wei-Ping Gai holds an Australian National Health and Medical Research Council (NHMRC) Fellowship, and this work was supported by the NHMRC Brain Bank of South Australia and Flinders Medical Foundation. Dr. Tong Chen has been supported by an Australian Postgraduate Award and more recently by an Australian Alzheimer's Research Dementia Fellowship. The authors would like to acknowledge the technical assistance of Xiao-Feng Shen and Fariba Chegini with the immunostaining, the help of Kylie Lange with the statistical analysis, and the helpful paper comments of Associate Professor Mark Gorrell and Professor Zhuo-Hua Zhang. This work was supported by the NHMRC Brain Bank of South Australia managed by Robyn Flook and Flinders Medical Foundation.

## References

[1] C. L. Masters, R. Cappai, K. J. Barnham, and V. L. Villemagne, "Molecular mechanisms for Alzheimer's disease: implications for neuroimaging and therapeutics," *Journal of Neurochemistry*, vol. 97, no. 6, pp. 1700–1725, 2006.

[2] D. J. Selkoe, "Alzheimer's disease is a synaptic failure," *Science*, vol. 298, no. 5594, pp. 789–791, 2002.

[3] J. Hardy, "A hundred years of Alzheimer's disease research," *Neuron*, vol. 52, no. 1, pp. 3–13, 2006.

[4] A. Goate, M.-C. Chartier-Harlin, M. Mullan et al., "Segregation of a missense mutation in the amyloid precursor protein gene with familial Alzheimer's disease," *Nature*, vol. 349, no. 6311, pp. 704–706, 1991.

[5] G. Thinakaran and S. S. Sisodia, "Presenilins and Alzheimer disease: the calcium conspiracy," *Nature Neuroscience*, vol. 9, no. 11, pp. 1354–1355, 2006.

[6] E. H. Corder, A. M. Saunders, W. J. Strittmatter et al., "Gene dose of apolipoprotein E type 4 allele and the risk of Alzheimer's disease in late onset families," *Science*, vol. 261, no. 5123, pp. 921–923, 1993.

[7] D. J. Selkoe, "Cell biology of protein misfolding: the examples of Alzheimer's and Parkinson's diseases," *Nature Cell Biology*, vol. 6, no. 11, pp. 1054–1061, 2004.

[8] S. Oddo, L. Billings, J. P. Kesslak, D. H. Cribbs, and F. M. LaFerla, "A$\beta$ immunotherapy leads to clearance of early, but not late, hyperphosphorylated tau aggregates via the proteasome," *Neuron*, vol. 43, no. 3, pp. 321–332, 2004.

[9] R. Etcheberrigaray, E. Ito, K. Oka, B. Tofel-Grehl, G. E. Gibson, and D. L. Alkon, "Potassium channel dysfunction in fibroblasts identifies patients with Alzheimer disease," *Proceedings of the National Academy of Sciences of the United States of America*, vol. 90, no. 17, pp. 8209–8213, 1993.

[10] H. A. de Silva, J. K. Aronson, D. G. Grahame-Smith, K. A. Jobst, and A. D. Smith, "Abnormal function of potassium channels in platelets of patients with Alzheimer's disease," *The Lancet*, vol. 352, no. 9140, pp. 1590–1593, 1998.

[11] N. H. Shah and E. Aizenman, "Voltage-gated potassium channels at the crossroads of neuronal function, ischemic tolerance, and neurodegeneration," *Translational Stroke Research*, vol. 5, no. 1, pp. 38–58, 2014.

[12] X. Wu, B. Hernandez-Enriquez, M. Banas, R. Xu, and F. Sesti, "Molecular mechanisms underlying the apoptotic effect of KCNB1 $K^+$ channel oxidation," *The Journal of Biological Chemistry*, vol. 288, no. 6, pp. 4128–4134, 2013.

[13] K. Yamamoto, Y. Ueta, L. Wang et al., "Suppression of a neocortical potassium channel activity by intracellular amyloid-$\beta$ and its rescue with homer1a," *Journal of Neuroscience*, vol. 31, no. 31, pp. 11100–11109, 2011.

[14] H. H. Jerng, P. J. Pfaffinger, and M. Covarrubias, "Molecular physiology and modulation of somatodendritic A-type potassium channels," *Molecular and Cellular Neuroscience*, vol. 27, no. 4, pp. 343–369, 2004.

[15] S. G. Birnbaum, A. W. Varga, L.-L. Yuan, A. E. Anderson, J. D. Sweatt, and L. A. Schrader, "Structure and function of Kv4-family transient potassium channels," *Physiological Reviews*, vol. 84, no. 3, pp. 803–833, 2004.

[16] M. S. Nadal, A. Ozaita, Y. Amarillo et al., "The CD26-related dipeptidyl aminopeptidase-like protein DPPX is a critical component of neuronal A-type $K^+$ channels," *Neuron*, vol. 37, no. 3, pp. 449–461, 2003.

[17] H. H. Jerng, K. Kunjilwar, and P. J. Pfaffinger, "Multiprotein assembly of Kv4.2, KChIP3 and DPP10 produces ternary channel complexes with ISA-like properties," *Journal of Physiology*, vol. 568, no. 3, pp. 767–788, 2005.

[18] M. Ikeda, D. Dewar, and J. McCulloch, "Preservation of [$^{125}$I]galanin binding sites despite loss of cholinergic neurons to the hippocampus in Alzheimer's disease," *Brain Research*, vol. 568, no. 1-2, pp. 303–306, 1991.

[19] M. Ramsden, Z. Henderson, and H. A. Pearson, "Modulation of $Ca^{2+}$ channel currents in primary cultures of rat cortical neurones by amyloid $\beta$ protein (1–40) is dependent on solubility status," *Brain Research*, vol. 956, no. 2, pp. 254–261, 2002.

[20] M. Ramsden, L. D. Plant, N. J. Webster, P. F. T. Vaughan, Z. Henderson, and H. A. Pearson, "Differential effects of unaggregated and aggregated amyloid $\beta$ protein (1–40) on $K^+$ channel currents in primary cultures of rat cerebellar granule and cortical neurones," *Journal of Neurochemistry*, vol. 79, no. 3, pp. 699–712, 2001.

[21] J. D. Buxbaum, E.-K. Choi, Y. Luo et al., "Calsenilin: a calcium-binding protein that interacts with the presenilins and regulates the levels of a presenilin fragment," *Nature Medicine*, vol. 4, no. 10, pp. 1177–1181, 1998.

[22] E.-K. Choi, N. F. Zaidi, J. S. Miller et al., "Calsenilin is a substrate for caspase-3 that preferentially interacts with the familial Alzheimer's disease-associated C-terminal fragment of presenilin 2," *The Journal of Biological Chemistry*, vol. 276, no. 22, pp. 19197–19204, 2001.

[23] D.-G. Jo, J.-Y. Lee, Y.-M. Hong et al., "Induction of pro-apoptotic calsenilin/DREAM/KChIP3 in Alzheimer's disease and cultured neurons after amyloid-$\beta$ exposure," *Journal of Neurochemistry*, vol. 88, no. 3, pp. 604–611, 2004.

[24] B. Coles, L. A. K. Wilton, M. Good, P. F. Chapman, and K. T. Wann, "Potassium channels in hippocampal neurones are absent in a transgenic but not in a chemical model of Alzheimer's disease," *Brain Research*, vol. 1190, no. 1, pp. 1–14, 2008.

[25] D. Liu, M. Pitta, J.-H. Lee et al., "The KATP channel activator diazoxide ameliorates amyloid-$\beta$ and Tau pathologies and improves memory in the 3xTgAD mouse model of Alzheimer's disease," *Journal of Alzheimer's Disease*, vol. 22, no. 2, pp. 443–457, 2010.

[26] T. Chen, D. Smyth, and C. A. Abbott, "CD26," *Journal of Biological Regulators and Homeostatic Agents*, vol. 18, no. 1, pp. 47–54, 2004.

[27] T. Chen, K. Ajami, G. W. McCaughan, W.-P. Gai, M. D. Gorrell, and C. A. Abbott, "Molecular characterization of a novel dipeptidyl peptidase like 2-short form (DPL2-s) that is highly expressed in the brain and lacks dipeptidyl peptidase activity," *Biochimica et Biophysica Acta*, vol. 1764, no. 1, pp. 33–43, 2006.

[28] H. H. Jerng, A. D. Lauver, and P. J. Pfaffinger, "DPP10 splice variants are localized in distinct neuronal populations and act to differentially regulate the inactivation properties of Kv4-based ion channels," *Molecular and Cellular Neuroscience*, vol. 35, no. 4, pp. 604–624, 2007.

[29] K. McNicholas, T. Chen, and C. A. Abbott, "Dipeptidyl peptidase (DP) 6 and DP10: novel brain proteins implicated in human health and disease," *Clinical Chemistry & Laboratory Medicine*, vol. 47, no. 3, pp. 262–267, 2009.

[30] C. A. Abbott, G. W. McCaughan, M. T. Levy, W. B. Church, and M. D. Gorrell, "Binding to human dipeptidyl peptidase IV by adenosine deaminase and antibodies that inhibit ligand binding involves overlapping, discontinuous sites on a predicted $\beta$ propeller domain," *European Journal of Biochemistry*, vol. 266, no. 3, pp. 798–810, 1999.

[31] K. Takimoto, Y. Hayashi, X. Ren, and N. Yoshimura, "Species and tissue differences in the expression of DPPY splicing variants," *Biochemical and Biophysical Research Communications*, vol. 348, no. 3, pp. 1094–1100, 2006.

[32] M. Allen, A. Heinzmann, E. Noguchi et al., "Positional cloning of a novel gene influencing asthma from Chromosome 2q14," *Nature Genetics*, vol. 35, no. 3, pp. 258–263, 2003.

[33] S. Y. Qi, P. J. Riviere, J. Trojnar, J.-L. Junien, and K. O. Akinsanya, "Cloning and characterization of dipeptidyl peptidase 10, a new member of an emerging subgroup of serine proteases," *Biochemical Journal*, vol. 373, no. 1, pp. 179–189, 2003.

[34] H. Vacher, D. P. Mohapatra, and J. S. Trimmer, "Localization and targeting of voltage-dependent ion channels in mammalian central neurons," *Physiological Reviews*, vol. 88, no. 4, pp. 1407–1447, 2008.

[35] E. Zagha, A. Ozaita, S. Y. Chang et al., "DPP10 modulates Kv4-mediated A-type potassium channels," *The Journal of Biological Chemistry*, vol. 280, no. 19, pp. 18853–18861, 2005.

[36] T. F. Gendron, "The role of tau in neurodegeneration," *Molecular Neurodegeneration*, vol. 4, no. 1, article 13, 2009.

[37] E. Braak, H. Braaak, and E.-M. Mandelkow, "A sequence of cytoskeleton changes related to the formation of neurofibrillary tangles and neuropil threads," *Acta Neuropathologica*, vol. 87, no. 6, pp. 554–567, 1994.

[38] K. Ikeda, C. Haga, S. Oyanagi, S. Iritani, and K. Kosaka, "Ultrastructural and immunohistochemical study of degenerate neurite-bearing ghost tangles," *Journal of Neurology*, vol. 239, no. 4, pp. 191–194, 1992.

[39] G. Lace, G. M. Savva, G. Forster et al., "Hippocampal tau pathology is related to neuroanatomical connections: an ageing population-based study," *Brain*, vol. 132, no. 5, pp. 1324–1334, 2009.

[40] S. Aronov, G. Aranda, L. Behar, and I. Ginzburg, "Axonal tau mRNA localization coincides with tau protein in living neuronal cells and depends on axonal targeting signal," *Journal of Neuroscience*, vol. 21, no. 17, pp. 6577–6587, 2001.

[41] M. A. Utton, J. Connell, A. A. Asuni et al., "The slow axonal transport of the microtubule-associated protein tau and the transport rates of different isoforms and mutants in cultured neurons," *Journal of Neuroscience*, vol. 22, no. 15, pp. 6394–6400, 2002.

[42] S. Konzack, E. Thies, A. Marx, E.-M. Mandelkow, and E. Mandelkow, "Swimming against the tide: mobility of the microtubule-associated protein tau in neurons," *Journal of Neuroscience*, vol. 27, no. 37, pp. 9916–9927, 2007.

[43] K. S. Kosik, "The molecular and cellular biology of tau," *Brain Pathology*, vol. 3, no. 1, pp. 39–43, 1993.

[44] J. Götz, L. M. Ittner, and S. Kins, "Do axonal defects in tau and amyloid precursor protein transgenic animals model axonopathy in Alzheimer's disease?" *Journal of Neurochemistry*, vol. 98, no. 4, pp. 993–1006, 2006.

[45] L. M. Ittner, Y. D. Ke, F. Delerue et al., "Dendritic function of tau mediates amyloid-$\beta$ toxicity in alzheimer's disease mouse models," *Cell*, vol. 142, no. 3, pp. 387–397, 2010.

[46] E. Magnani, J. Fan, L. Gasparini et al., "Interaction of tau protein with the dynactin complex," *The EMBO Journal*, vol. 26, no. 21, pp. 4546–4554, 2007.

[47] L. M. Ittner and J. Götz, "Amyloid-$\beta$ and tau—a toxic pas de deux in Alzheimer's disease," *Nature Reviews Neuroscience*, vol. 12, no. 2, pp. 67–72, 2011.

[48] W. Wong, E. W. Newell, D. G. M. Jugloff, O. T. Jones, and L. C. Schlichter, "Cell surface targeting and clustering interactions between heterologously expressed PSD-95 and the Shal voltage-gated potassium channel, Kv4.2," *The Journal of Biological Chemistry*, vol. 277, no. 23, pp. 20423–20430, 2002.

[49] W. Wong and L. C. Schlichter, "Differential recruitment of Kv1.4 and Kv4.2 to lipid rafts by PSD-95," *The Journal of Biological Chemistry*, vol. 279, no. 1, pp. 444–452, 2004.

[50] D. A. Hoffman, J. C. Magee, C. M. Colbert, and D. Johnston, "$K^+$ channel regulation of signal propagation in dendrites of hippocampal pyramidal neurons," *Nature*, vol. 387, no. 6636, pp. 869–875, 1997.

[51] Z. Lei, P. Deng, Y. Li, and Z. C. Xu, "Downregulation of Kv4.2 channels mediated by NR2B-containing NMDA receptors in cultured hippocampal neurons," *Neuroscience*, vol. 165, no. 2, pp. 350–362, 2010.

[52] C. Chen, "$\beta$-amyloid increases dendritic $Ca^{2+}$ influx by inhibiting the A-type $K^+$ current in hippocampal CA1 pyramidal neurons," *Biochemical and Biophysical Research Communications*, vol. 338, no. 4, pp. 1913–1919, 2005.

[53] T. Chen, K. Ajami, G. W. McCaughan, M. D. Gorrell, and C. A. Abbott, "Dipeptidyl peptidase IV gene family: the DPIV family," in *Advances in Experimental Medicine and Biology*, M. Hildebrandt, Ed., vol. 524, pp. 79–86, Kluwer/Plenum, New York, NY, USA, 2003.

[54] M. D. Gorrell, "First bite," *Nature Structural Biology*, vol. 10, no. 1, pp. 3–5, 2003.

[55] H.-L. Li, Y.-J. Qu, C. L. Yi et al., "DPP10 is an inactivation modulatory protein of Kv4.3 and Kv1.4," *American Journal of Physiology*, vol. 291, no. 5, pp. C966–C976, 2006.

[56] L. Lin, W. Sun, B. Throesch et al., "DPP6 regulation of dendritic morphogenesis impacts hippocampal synaptic development," *Nature Communications*, vol. 4, article 2270, 2013.

[57] R. C. Mercer, L. Ma, J. C. Watts et al., "The prion protein modulates A-type $K^+$ currents mediated by Kv4.2 complexes through dipeptidyl aminopeptidase-like protein 6," *The Journal of Biological Chemistry*, vol. 288, no. 52, pp. 37241–37255, 2013.